Nonlinear Technique for Energy Exchange Optimization in Piezoelectric Actuators

Benjamin Ducharne, Lauric Garbuio, Mickael Lallart, Daniel Guyomar, Gaël Sebald, Jean-Yves Gauthier

Nonlinear technique for energy exchange optimization in piezoelectric actuators.

B. DUCHARNE[1,a], L. GARBOUIO, M. LALLART, D. GUYOMAR[1], G. SEBALD[1], and JY. GAUTHIER

[1] Laboratoire de Génie Electrique et Ferroélectricité – INSA de Lyon

Bât. Gustave FERRIE, 8 rue de la physique, 69621 Villeurbanne cedex, FRANCE

ABSTRACT:

Applications of piezoelectric actuators have increased dramatically during the past decades. However, the capacitive nature of such devices makes their use delicate, especially in terms of power supply, as the instantaneous power may be much greater than the average effective power. The present paper places particular focus on the description of a nonlinear technique for piezoelectric actuator control. This technique enables to significantly increase the energy transfer efficiency of the device by reducing the reactive part of the power. Such an approach has the inverse effect of the well-known Synchronized Switch Damping (SSD) technique developed to reduce vibrations in smart structures. The proposed solution consists in disconnecting the driving voltage source from the piezoelectric element and switching the system to a passive electrical network at each occurrence of a voltage extremum. This switching strategy is designed to annihilate the reactive energy supplied by the voltage source and to decrease the active energy while ensuring a constant output power. Suppressing the reactive energy is particularly interesting for limiting the dimensions and energy requirements of power supplies. Compared to classical methods, the direct supply of both simulations and experimental validations has demonstrated the effectiveness of the proposed technique for eliminating all of the reactive energy and reducing the active power at frequencies close to the resonant one, while maintaining similar mechanical performances.

KEYWORDS:
Piezoelectric actuators, nonlinear, control system, reactive energy, active energy.

INTRODUCTION

The interest in ferroelectric properties, materials and devices has been considerable over the last 20 years. Reactive power and power factor correction have recently been the subject of numerous investigations [1]-[6]. Due to their specific electromechanical properties, piezoelectric materials are widely used as sensors and actuators. Piezoelectric ceramics are the dominant transduction materials in sonar and ultrasonic applications. The analysis of the power limitations of transducers has been discussed by Woollett [7]-[8] and Berlincourt [9]. There are three types of limitations:

_ The mechanical limits are caused by different factors such as fracture in the case of ceramic transducers, or metal fatigue.

_ The thermal limit is the consequence of energy dissipation. The thermally limited power output not only depends on the dielectric losses but also on the mechanical losses and the heat transfer design of the transducer.

_ The electrical limits are essentially related to the active material, and involve insulation breakdown or depolarization of the materials resulting from ferroelectric nonlinearities.

In addition to all these limitations, others originate from the electrical power supply. Because of the capacitive behavior of piezoceramic transducers, power amplifiers always need to supply high levels of reactive power, or equivalently high power peaks compared to average power, leading to an overdesign of power amplifiers by piezoceramic transducer manufacturers.

In a simple alternating current (AC) circuit consisting of a source and a linear load, both the current and voltage are sinusoidal. If the load is purely resistive, the two quantities reverse their polarity at the same time. At every instant, the product of voltage and current is positive, indicating that the direction of energy flow is not reversed. In this case, only real power is transferred.

If the loads are purely reactive, then the voltage and current are 90 degrees out of phase.

For half of each cycle, the product of voltage and current is positive, but on the other half of the cycle, the product is negative, indicating that on average, exactly as much energy flows toward the load as back from it. There is no net energy flow over one cycle. In this case, there is only a flow of reactive energy and there is no net transfer of energy load.

Practical loads have resistance, inductance, and capacitance, so both real and reactive powers will flow to read loads (Fig. 1a). Power engineers measure apparent power as the magnitude of the vector sum of real and reactive powers. The apparent power is the product of the root-mean-square of voltage and current.

Engineers use the following terms to describe energy flow in a system (and assign each of them a different unit to differentiate between them):

_ Real power (P) or active power: watt (W)

_ Reactive power (Q): volt-ampere (VA)

_ Complex power (S): volt-ampere (VA)

_ Apparent power ($|S|$) (absolute value of complex power S: volt-ampere (VA).

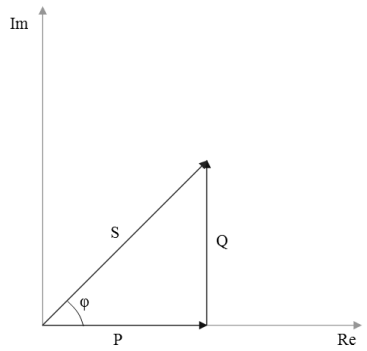

Fig. 1a – Vector scheme of complex power.

This study presents the development of a new nonlinear technique for controlling piezoelectric transducers which enables to decrease this reactive energy and increase the energy transfer performance in the system.

The technique is based on recent developments in the fields of vibration control and

energy harvesting [10]-[16]. Semi-active vibration control techniques through nonlinear treatments have experienced significant progress over the last years, due to their effectiveness and advantages compared to passive and active approaches. In particular, the so-called Synchronized Switch Damping (SSD) technique permits a very effective reduction of the vibrations thanks to an artificial increase of the coupling coefficient caused by a particular nonlinear processing of the voltage output of the piezoelectric transducer [17]-[19]. This nonlinear approach consists in connecting the active material to an electric network for a brief time period. This connection leads to an inversion of the piezovoltage which induces a cumulative effect. It magnifies the voltage magnitude while shifting also this voltage, yielding a significant increase of the energy conversion abilities.

This paper presents an inverse approach of the SSD technique. The objective of this study was to increase the piezoelectric actuator performances. A nonlinear treatment of the electrical actuator suppliers enables to notably reduce the energy consumption without significantly modifying the mechanical characteristics. The first priority of this study was to minimize the reactive energy and the high instantaneous power usually required for actuating the device. A marked decrease of this energy leads to a high reduction of the electrical currents provided by power amplifiers. The consequences of such reductions involve new opportunities for designing ultra-compact, low-cost power amplifiers for piezoceramic actuators.

The second priority of the study was to decrease the required active power close to the resonant frequency (where piezoelectric actuators are classically used). By enhancing the energy exchange in the system, higher performances can be obtained with existing actuators, and new actuators of reduced dimensions can be developed to accomplish identical operations. To render possible the most extensive use of this new technique, the nonlinear treatment must be simple, easily transferable and based on a reduced number of

components.

This paper is organized in three parts. First, the objectives, principles and theoretical performances of the nonlinear driving approach are exposed in Section 2. Section 3 then provides an experimental investigation aiming at validating the proposed concept. Finally, Section 4 concludes the study.

II. BASIC THEORY AND MODELING

II.1 Smart structure modeling

Lumped model analysis of smart structures has received considerable attention since the seventies, and the formulation presented by Alik and Hughes [20], based on the variational principle, is widely referenced. For simplicity, the model used in this paper involves one piezoelectric element and has one degree of freedom. Indeed, a mechanical model based on only one degree of freedom gives a good description of the vibrating structure behavior near one of its resonant frequencies. Close to one of the resonant frequencies, the dynamic behavior and governing equations of the structure can therefore be written as:

$$M\ddot{u} + C\dot{u} + K^E u = -\alpha V \tag{1}$$

$$I = \alpha\dot{u} - C_0\dot{V} \tag{2}$$

where u is the displacement of the structure; M, C and K^E are, respectively, the mass, damping and stiffness when the piezoelectric element is short-circuited; α is the electromechanical coupling coefficient; V is the piezoelectric element voltage; I is the piezoelectric element current; and C_0 is the clamped capacitance.

In an open circuit, the current is null, therefore Eq. (2) becomes:

$$V = \frac{\alpha.u}{C_0} \tag{3}$$

II.2 Basic theory of the nonlinear piezoelectric control

The aim of the nonlinear piezoelectric actuator control is to create a driving effect without any knowledge of the structure characteristics. The method consists of disconnecting the piezoelement from the driving source when the latter reaches a maximal or minimal value (*Sw1*), while switching it to an inductor (*Sw2* – Fig. 2), therefore forming a resonant electrical network. This switching operation is repeated each half period, where the switch is closed during half of the pseudo-period of the electrical oscillating network. The switching time instants are precisely defined so as to minimize the reactive energy provided by the power amplifier and to maximize the relative active energy conversion. The resonant electrical network is constituted by an inductance L connected in series with the digital switch.

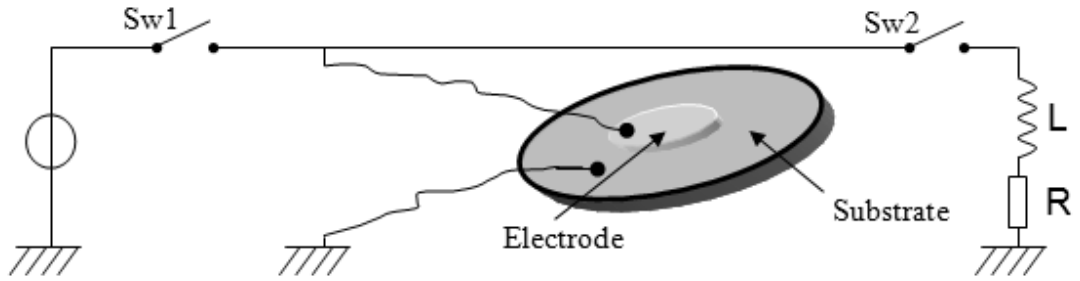

Fig. 2a – Experimental structure.

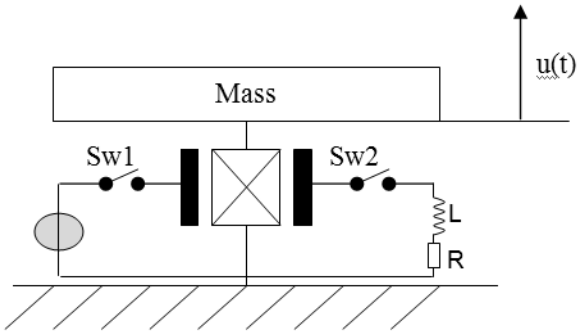

Fig. 2b – Single degree of freedom (SDOF) model.

The description of the process starts with the following initial conditions:

_ The voltage source value is zero.

_ The equivalent capacitor of the piezoelectric element is unloaded.

First, when the driving voltage is increasing but still lower than its maximum value, the electric source is connected to the piezoelectric element (*sw1* closed, *sw2* open), and energy is transferred from the electric power supply to the electromechanical converter. The associated electric circuit is displayed in Fig.3.

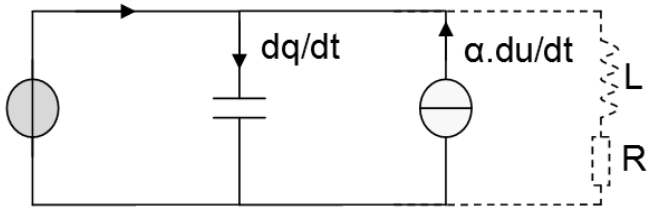

Fig. 3 – Electrical circuit for the first step of the process.

The constitutive equations during this process are thus given as:

$$M.\ddot{u} + C.\dot{u} + K.u = -\alpha.V \tag{5}$$

$$I = \dot{q} - \alpha.\dot{u} \tag{6}$$

When the electrical source reaches a maximum (or a minimum) value, *sw1* is open and *sw2* is closed. The piezoelectric element is then connected to the electrical network (constituted by the actuator and the inductance *L* - whose internal resistance is given by *r* - in series with the digital switch *sw2*), shaping a resonant network because of the capacitive behavior of the piezoelectric material.

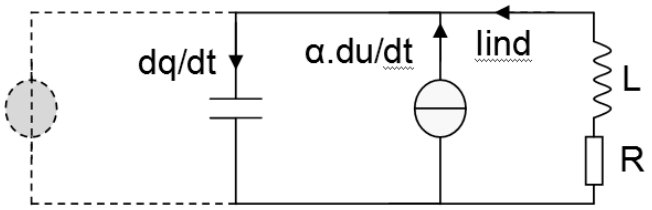

Fig. 4 – Electrical circuit for the second step of the process.

In this case, the constitutive equations become:

$$M.\ddot{u} + C.\dot{u} + K.u = -\alpha.V \tag{7}$$

$$I_{ind} = \dot{q} - \alpha.\dot{u} \tag{8}$$

$$L.\ddot{q}_{ind} + R.\dot{q}_{ind} + \frac{1}{C_0}\left(q_{ind} + \alpha.u\right) = 0 \tag{9}$$

The electrical circuit remains in this configuration as long as the piezoelectric element voltage is different from that of the source. When the two voltages are equal, the switches return to their initial conditions (*sw1* closed, *sw2* open), and a new cycle begins.

II.3 Energy transfers of the nonlinear control technique

The main objective of the nonlinear technique is to provide an equivalent mechanical effect with a reduced consumption of active power and a full suppression of the reactive power at working frequencies close to the resonant one. During the first phase of the process, the energy transfers can be described with the following equations:

$$\int_0^{\sigma.\frac{T}{2}} M.\ddot{u}.\dot{u}.dt + \int_0^{\sigma.\frac{T}{2}} C.\dot{u}^2.dt + \int_0^{\sigma.\frac{T}{2}} K.u.\dot{u}.dt = \int_0^{\sigma.\frac{T}{2}} -\alpha.V.dt \tag{10}$$

$$\int_0^{\sigma.\frac{T}{2}} I.V.dt = \int_0^{\sigma.\frac{T}{2}} \dot{q}.V.dt - \int_0^{\sigma.\frac{T}{2}} \alpha.\dot{u}.V.dt \tag{11}$$

Here, $\int_0^{\sigma.\frac{T}{2}} M.\ddot{u}.\dot{u}.dt$ is the kinetic energy, $\int_0^{\sigma.\frac{T}{2}} C.\dot{u}^2.dt$ the mechanical losses, and $\int_0^{\sigma.\frac{T}{2}} K.u.\dot{u}.dt$ the potential energy. Moreover, T is the voltage source period and σ is the duty cycle defined as:

$$t \in \left[0; \sigma\frac{T}{2}\right] \cup \left[\frac{T}{2}; \frac{T}{2} + \sigma\frac{T}{2}\right] \qquad t \in \left[\sigma\frac{T}{2}; \frac{T}{2}\right] \cup \left[\frac{T}{2} + \sigma\frac{T}{2}; T\right]$$

$$sw_1 = 1; sw_2 = 0 \qquad sw_1 = 0; sw_2 = 1$$

$\int_0^{\sigma.\frac{T}{2}} I.V.dt$ is the electrical energy provided by the power amplifier. Identical equations have been established for the second phase of the process yielding:

$$\int_{\sigma.\frac{T}{2}}^{\frac{T}{2}} M.\ddot{u}.\dot{u}.dt + \int_{\sigma.\frac{T}{2}}^{\frac{T}{2}} C.\dot{u}^2.dt + \int_{\sigma.\frac{T}{2}}^{\frac{T}{2}} K.u.\dot{u}.dt = \int_{\sigma.\frac{T}{2}}^{\frac{T}{2}} -\alpha.V.dt \tag{12}$$

$$\int_{\sigma.\frac{T}{2}}^{\frac{T}{2}} I_{ind}.\frac{q}{c_0}.dt = \int_{\sigma.\frac{T}{2}}^{\frac{T}{2}} \dot{q}.\frac{q}{c_0}.dt - \int_{\sigma.\frac{T}{2}}^{\frac{T}{2}} \alpha.\dot{u}.\frac{q}{c_0}.dt \tag{13}$$

Finally, during an entire semi-excitation period, the energy supplied by the electric amplifier is given by:

$$\int_0^{\sigma.\frac{T}{2}} I.V.dt \tag{14}$$

II.4 Model of the piezoelectric actuator with the nonlinear control technique

A complete switching process model has been developed using the previous constitutive equations. The test structure employed in the simulation is similar to the experimental one and consists of a circular piezoelectric buzzer lightly clamped at its edge by a plastic support, as shown in Fig. 5.

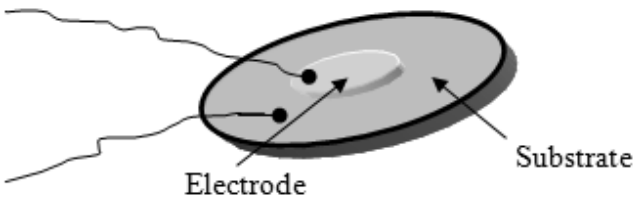

Fig. 5 – Piezoelectric buzzer.

The nonlinear technique is modeled using the previous equations. The simulation time step has been set sufficiently low so as not to lose information. A laboratory-developed Runge Kuntta 4 (RK4) algorithm is implemented in Matlab in order to assess the performance of the technique through simulations.

The piezoelectric parameters of the actuator have been characterized and are summarized in Tab.1.

Dynamic mass M	1.10^{-3} Kg
Structural damping coefficient C	0.02 N s m^{-1}
Open circuit stiffness K^D	1.10^{3} N m^{-1}
Force factor α	-1.10^{-3}N V^{-1}
Clamped capacitance C_0	30 nF
Coupling factor	0.18

Tab. 1 – Identification of the experimental parameters.

Fig. 6 shows the voltage evolutions. When the source voltage is different from that of the piezo, the buzzer is connected to the inductance. This figure illustrates the piezoceramic voltage variations during the different steps of the process. The inductor value sets the frequency of the piezoceramic voltage inversion when it is disconnected from the voltage source. By adjusting this frequency, the power consumption by the actuator can be optimized.

Other losses, for instance switching losses, may be neglected compared to those of the inductor. For instance, for a typical gate-source input capacitance of *25* pF with a driving frequency of *1* kHz and a gate voltage of *12* V, the corresponding power consumption would be 3.6 µW. On the other hand, the resistive losses in the switching branch would be *474* µW for a *10* V input voltage, with a piezocapacitance of *30* nF, an inductance value of *100* mH and a series resistance of the switching branch of *100* Ω.

In addition, the drain-source capacitor may also be neglected compared to the piezoelement capacitance, although it may generate high frequency oscillations (which are however not prejudicial for the system) when the switch is turned on and off. The inductor value has been set in order to match the half period of the resonant instant (when the piezo voltage reaches its maximum) with the instant where the voltage of the source and of the piezo are equal. The objective is to minimize the energy losses, which appear at the disconnecting time of the inductor. This minimization corresponds to a minimization of the energy consumption, which is the objective. In the case of the piezoelectric buzzer actuator, the capacitance of the piezo-element is close to 30 nF. The best performances are obtained with an inductor value of 240 mH.

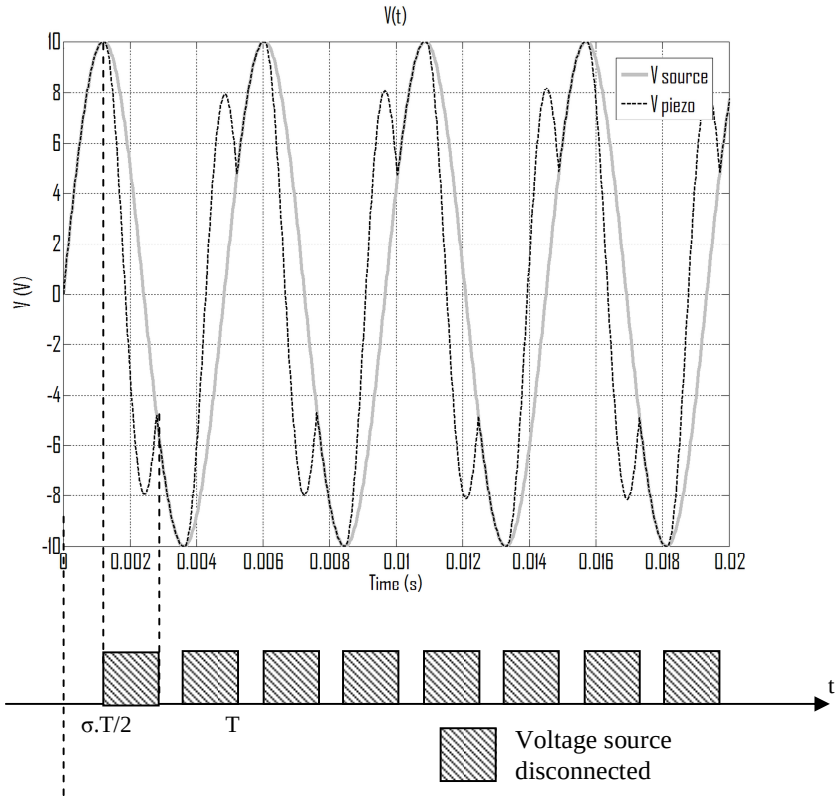

Fig. 6 – Simulation plot of the circuit voltages.

The second set of simulation results are displayed in Fig.7. Fig.7.a shows the variation of current through the clamped capacitance of the piezoelectric actuator versus time, with a dashed line for the case without control and solid grey for the case with a control process. We can here observe the discontinuities caused by the commutation. Fig.7.b exhibits the generator current, Fig.7.c the source voltage and Fig.7.d the buzzer displacement. By comparing Fig.7.b and 7.c, we can confirm that the generator current and its voltage always have the same sign hence preventing reactive energy in the system, which is not true in the case without control.

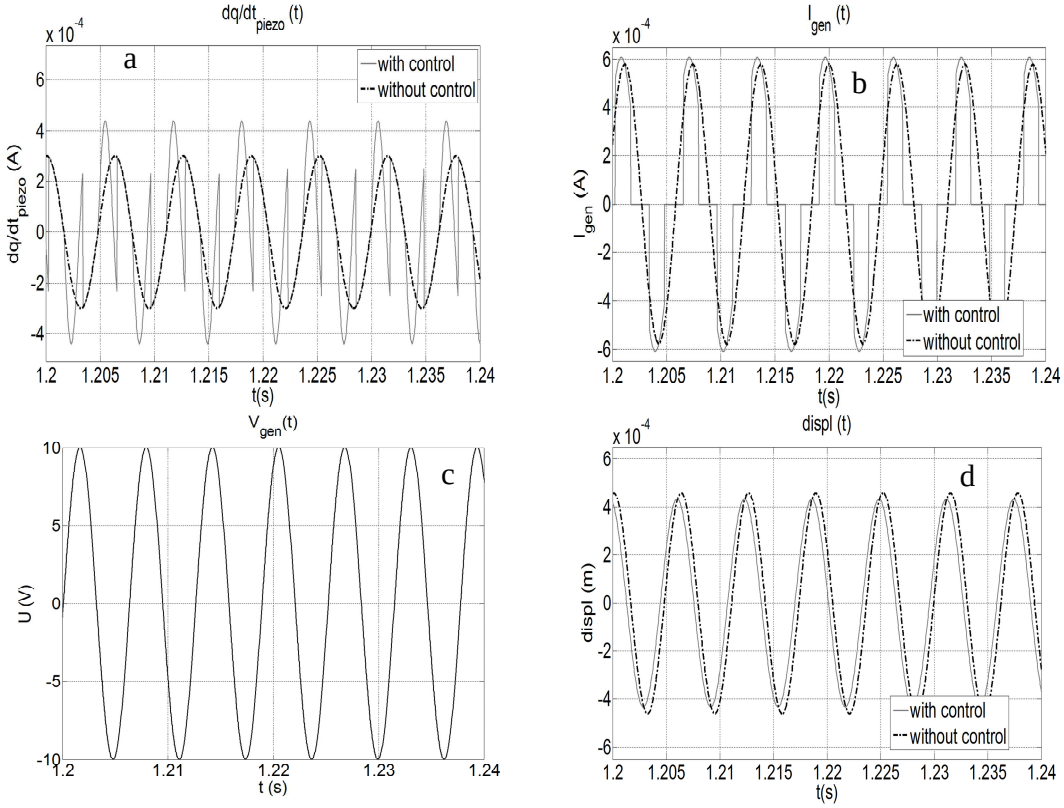

Fig. 7 – Simulation results.

Fig.8 displays the instantaneous power provided by the amplifier. This plot confirms the total suppression of the reactive energy. In other words, the instantaneous power is

always positive.

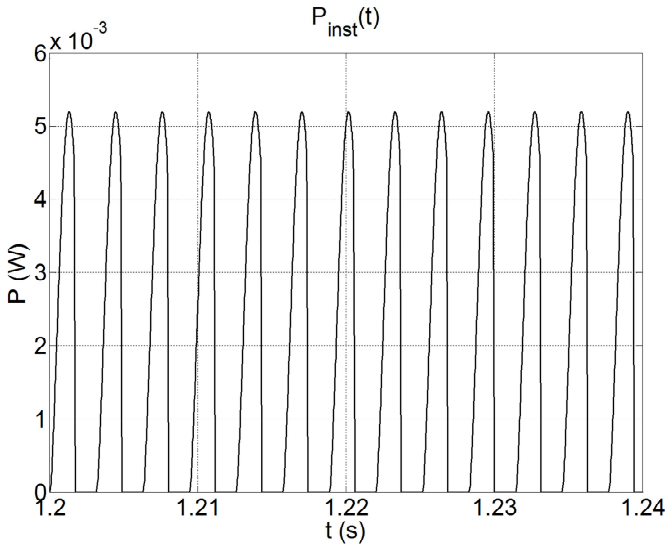

Fig. 8 – Simulation results.

III. EXPERIMENTAL RESULTS

III.1 Experimental setup

An overview of the experimental setup is shown in Fig. 9a, in which the experimental sample is the circular piezoelectric buzzer described previously. The monitoring of the device center displacement is performed by means of an optical laser vibrometer (Polytec OFV 5000 vibrometer controller), the piezoelectric buzzer is driven by a frequency generator (Agilent 33220 A), and MOSFET transistors (2N7000) have been used for the switching device. All measuring signals (from the piezoelectric element and vibrometer) are simply monitored using an oscilloscope (Agilent DSO7034A). The signal processing for the command and switch control is performed by a Dspace digital/analog real time controller. The simulink schemes are displayed in the Fig. 9b.

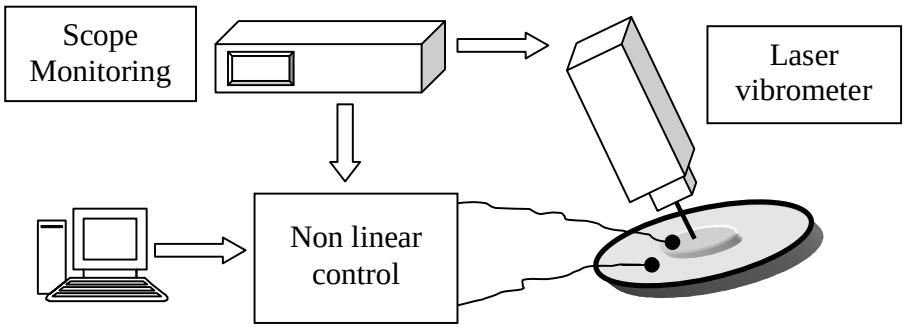

Fig. 9.a – Experimental test structure.

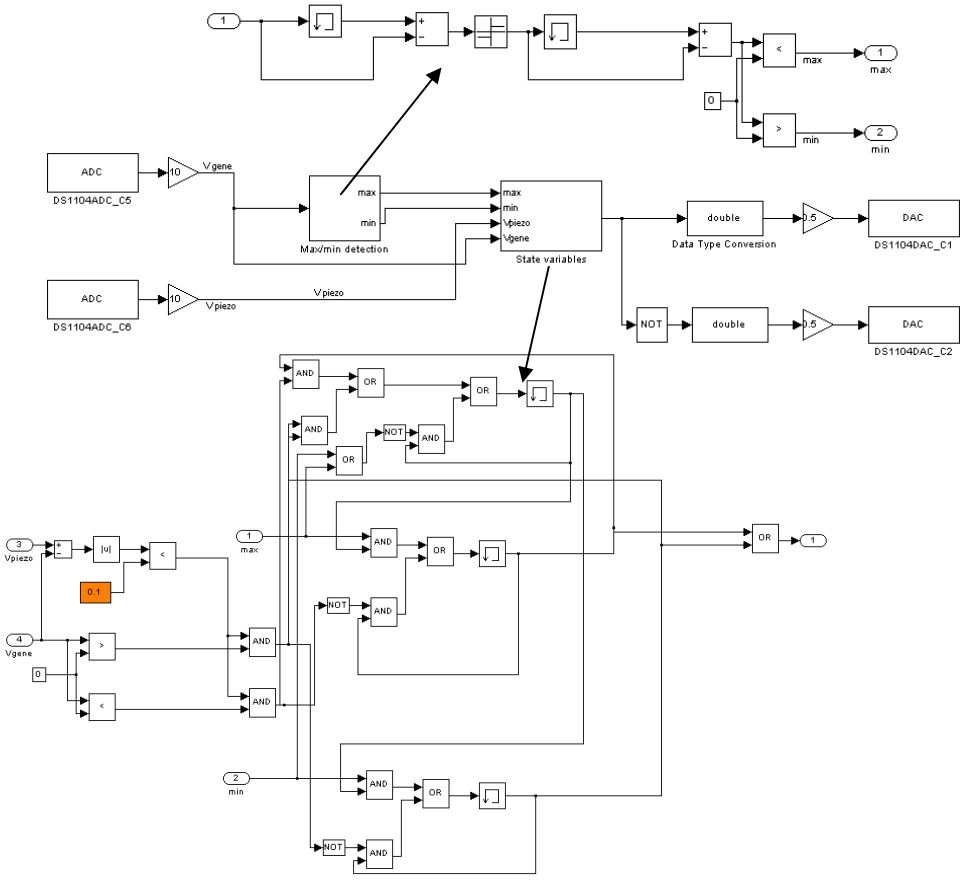

Fig. 9.b – Simulink schemes of the switches control.

Furthermore, floating switches have been developed especially to electrically disconnect the switch command from the generator as well as connecting the material to the inversion branch. The electronic specifications of the switches are detailed in Fig. 9c:

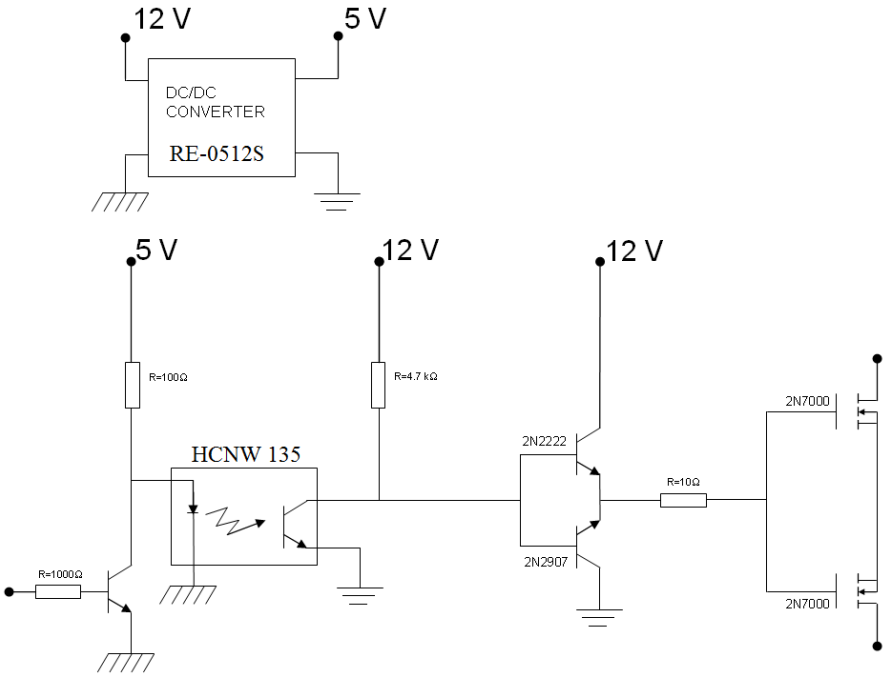

Fig. 9.c – Electronic scheme of implemented switches.

III.2 Experimental results

Fig. 10 presents the first experimental curves of the voltage versus time. The analysis of this figure leads to the conclusion that the control of the switching is correctly done, and that the driving time of the piezoelectric element by the source supplier is similar to the simulated one. The amplifier remains disconnected during almost half the voltage source period which justifies the reduction of the power consumption.

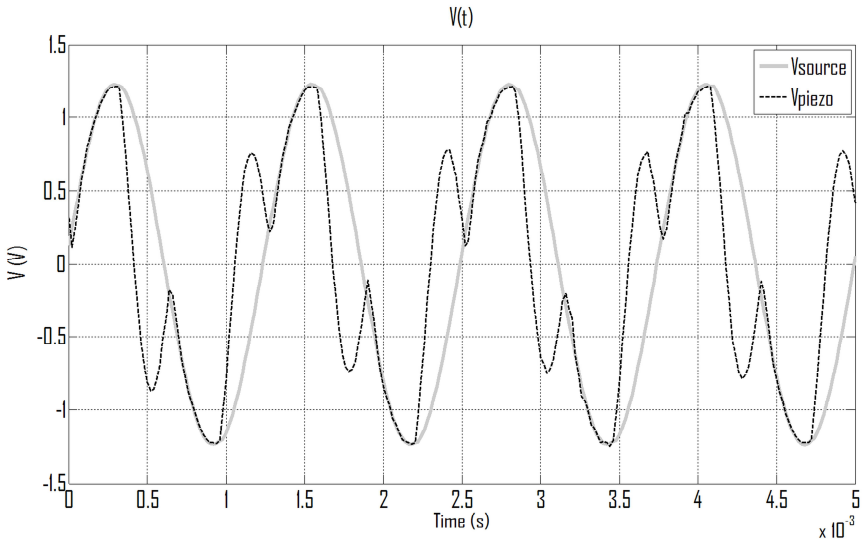

Fig. 10 – Experimental variations of the circuit voltages.

Fig. 11 shows the instantaneous power provided by the voltage source. We confirm here that, as observed for the simulations, this curve is always positive and that all reactive components of the power have been suppressed. Fig. 11 exhibits a small resonant behavior at the switching instant, probably due to the parasitic capacitance of the transistor.

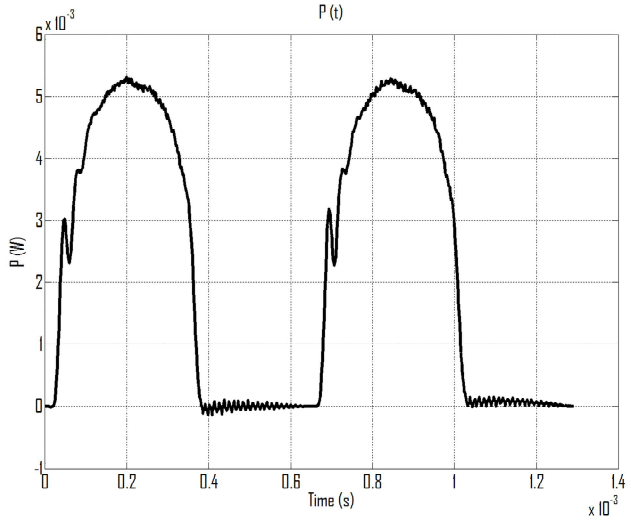

Fig. 11 – Experimental test structure.

Fig. 12 shows the experimental and simulated energies supplied by the amplifier versus frequency. In particular, we notice that the nonlinear technique significantly reduces the energy consumption at frequencies close to the resonant one. This observation is however not true for the remaining spectrum where this tendency is inversed (i.e., the energy consumption with switch control is higher than the energy consumption without switch control). In Fig. 12.A and 13.A, the damping coefficient C is equal to 0.02, while it is equal to 0.05 in Fig. 12.B and 13.B. By increasing this coefficient, we increase the mechanical load of the piezoelectric buzzer, which corresponds to a shift of the resonant frequency (to low frequencies) and an enlargement of the peak. The damping coefficient can be modified experimentally by changing the piezo-actuator environment.

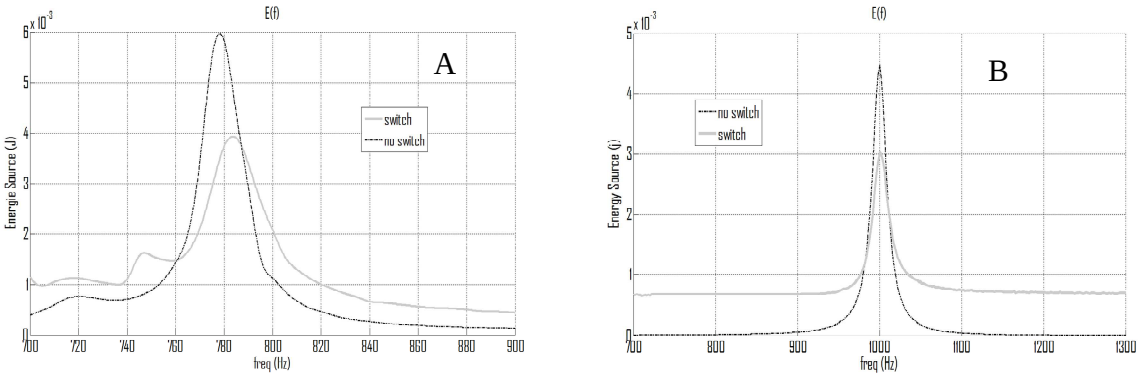

Fig. 12 – Source energy versus frequency (A - C=0.05; B - C=0.02).

Fig. 13 shows the experimental and the simulated variations of the maximum displacement versus the frequency with and without the use of the nonlinear technique for the same frequency bandwidth.

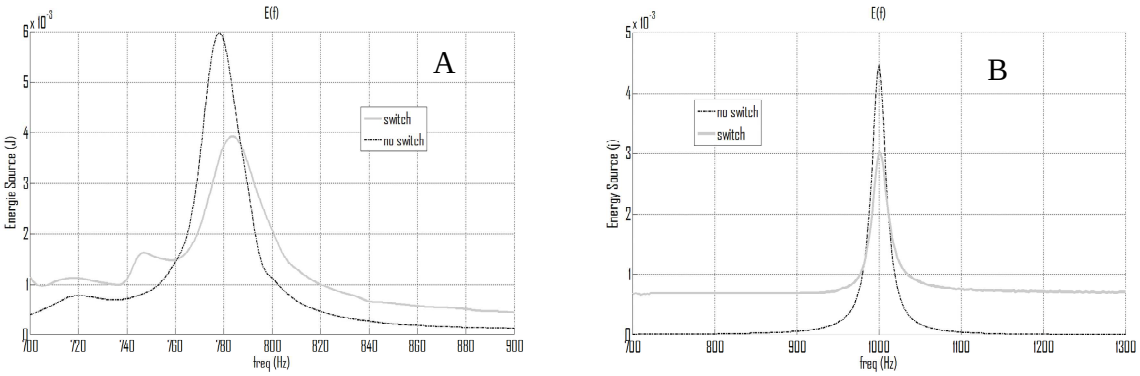

Fig. 13 – Displacement versus frequency (A - C=0.05; B - C=0.02).

We can notice here that the displacement is almost similar, which means that the electromechanical properties of the buzzer are not significantly modified by the nonlinear control technique.

The energy consumption at the power amplifier output has been calculated in simulation by integrating a hundred periods of the instantaneous power. This instantaneous power is taken as the product of the amplifier voltage and the electrical current. Far from the resonant frequency, the energy consumption measured at the power amplifier output clearly becomes higher when using the nonlinear control technique. This difference is mainly due to the pure capacitive behavior of the piezoceramic. It is also due to the switching losses, which appear in the control process, and to the resistance of the inductance.

Without nonlinear control, the instantaneous energy exhibits an average value close to zero. By taking into account the internal resistor consumption of the power amplifier (whose value is 50Ω), this difference is clearly reduced (as illustrated in Fig. 14). To correctly compare the energy consumptions far from the resonant frequency, it is necessary to take into account the active energy consumptions of all the electrical distribution chains, i.e., from the production step to the buzzer consumption. By correctly calculating the total energy consumption, it is possible that the final energy consumption under nonlinear control can be lower than with classical control.

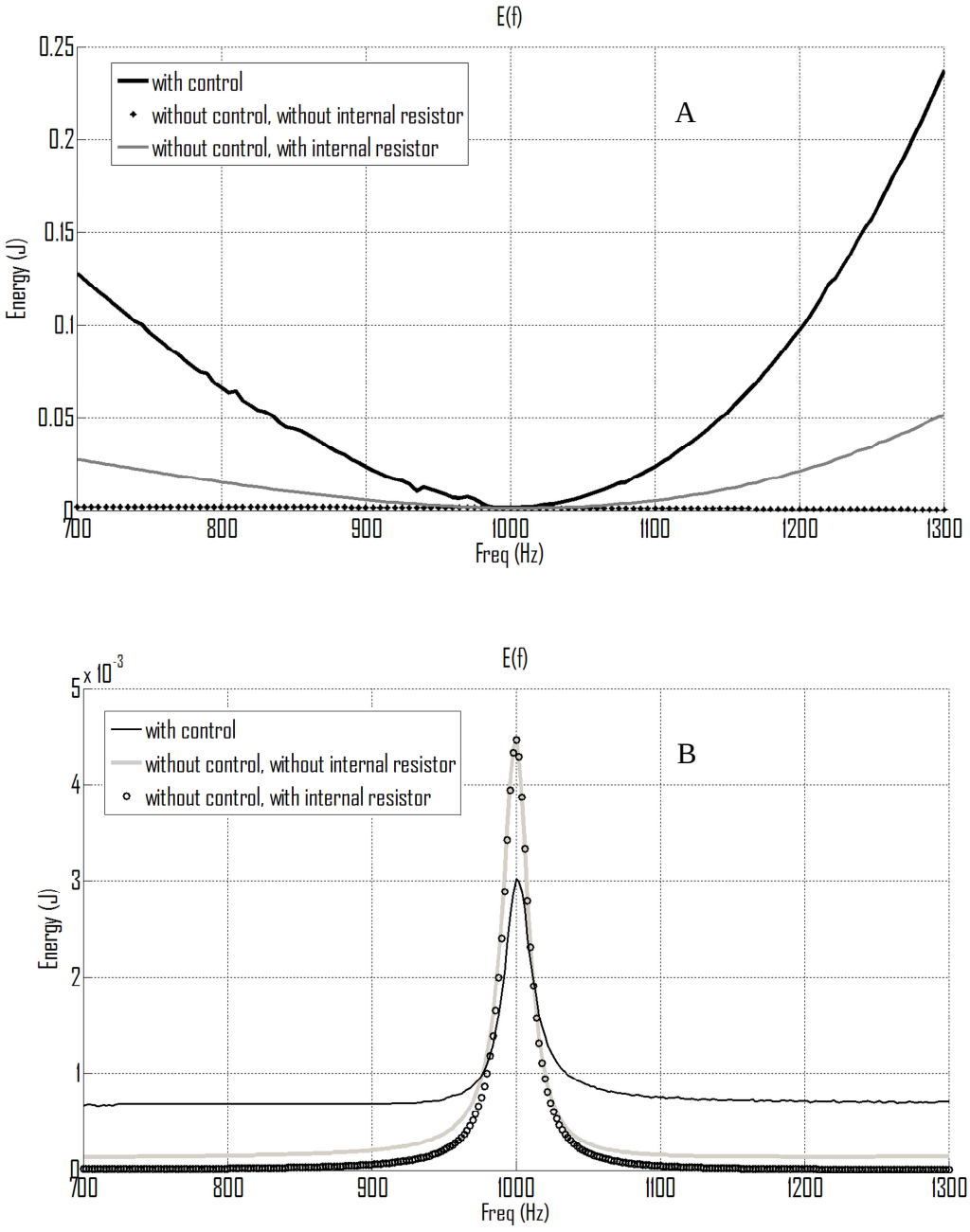

Fig. 14 – Influence of the amplifier internal resistor on the energy consumption (A - at constant displacement B - at constant amplifier voltage).

All the energy consumptions of the direct and nonlinear control are resumed in Tab. 2.

	Energy (j) at the amplifier output			
	freq (Hz)	Direct control		Nonlinear control
		with internal resistor	Without internal resistor	
At constant displacement	800	0,0154	0,0023	0,06
	900	0,006	0,002	0,0236
	1000	0,0015	0,0013	0,0013
	1100	0,0057	0,0015	0,0236
	1200	0,02	0,0011	0,097
At constant amplifier voltage	800	1,62E-05	0,00015	0,00068
	900	5,70E-05	0,0002	0,00068
	1000	0,0045	0,0045	0,003
	1100	4,30E-05	0,00016	0,000753
	1200	9,03E-06	0,00014	0,000718

Close to the resonant frequency

Far from the resonant frequency

Tab. 2 – Comparison of energy

consumption between direct control and nonlinear control.

CONCLUSIONS

This paper proposes a new nonlinear control law to increase the energy transfer performances of piezoelectric transducers. The technique is based on a periodic switching of the piezoelement to an electrical network. This approach is independent of the electromechanical structure characteristics, thus allowing very large frequency band operations and a good robustness under environmental changes.

The proposed control law presents a very simple command that can be easily implemented. The proposed solution consists of disconnecting the voltage source and replacing it by a passive electrical network. The switching periods are chosen in order to annihilate the reactive energy supplied by the voltage source and to decrease the active power. Suppressing reactive energy is particularly interesting for the design of compact and efficient power supplies.

Experimental measurements have been carried out to validate the efficient suppression of the reactive energy by the nonlinear method. Near the resonant frequency, experimental results confirmed that the use of the nonlinear technique enabled a high reduction of the energy consumption close to the resonant frequency (usual operating frequency). Indeed,

close to the resonant frequency, the active energy is divided by two and the mechanical performances are maintained.

Although the nonlinear technique may not have a significant impact on the behavior of closed-loop systems as it only assists the power supply, the effect of the nonlinearities on such plants may be further investigated in future studies.

References

[1] M. Narimani and G. Moschopoulos, “A new single-phase single-stage three-level power factor correction ac-dc converter,” in *2011 Twenty-Sixth Annual IEEE Applied Power Electronics Conference and Exposition (APEC)*, 2011, pp. 48 –55.

[2] X. Xie, J. Wang, C. Zhao, Q. Lu, and S. Liu, “A Novel Output Current Estimation and Regulation Circuit for Primary Side Controlled High Power Factor Single-Stage Flyback LED Driver,” *IEEE Transactions on Power Electronics*, vol. 27, no. 11, pp. 4602 –4612, Nov. 2012.

[3] R. L. de Araujo Ribeiro, C. C. de Azevedo, and R. M. de Sousa, “A Robust Adaptive Control Strategy of Active Power Filters for Power-Factor Correction, Harmonic Compensation, and Balancing of Nonlinear Loads,” *IEEE Transactions on Power Electronics*, vol. 27, no. 2, pp. 718 –730, Feb. 2012.

[4] B. A. Mather and D. Maksimovic&#x0301 and, “A Simple Digital Power-Factor Correction Rectifier Controller,” *IEEE Transactions on Power Electronics*, vol. 26, no. 1, pp. 9 –19, Jan. 2011.

[5] Y.-S. Roh, Y.-J. Moon, J.-C. Gong, and C. Yoo, “Active Power Factor Correction (PFC) Circuit With Resistor-Free Zero-Current Detection,” *IEEE Transactions on Power Electronics*, vol. 26, no. 2, pp. 630 –637, Feb. 2011.

[6] D. G. Lamar, J. Sebastian, M. Arias, and A. Fernandez, “On the Limit of the Output Capacitor Reduction in Power-Factor Correctors by Distorting the Line Input Current,” *IEEE Transactions on Power Electronics*, vol. 27, no. 3, pp. 1168 –1176, Mar. 2012.

[7] R. S. Woollett, “Theoretical Power Limits of Sonar Transducers,” in *1962 IRE National Convention*, 1962, pp. 90 – 94.

[8] R. S. Woollett, “Power Limitations of Sonic Transducers,” *IEEE Transactions on Sonics and Ultrasonics*, vol. 15, no. 4, pp. 218 –228, Oct. 1968.

[9] W. P. Mason, *Physical acoustics: principles and methods*. Academic Press, 1976.

[10] A. Badel, G. Sebald, D. Guyomar, M. Lallart, E. Lefeuvre, C. Richard, and J. Qiu, “Piezoelectric vibration control by synchronized switching on adaptive voltage sources: Towards wideband semi-active damping,” *The Journal of the Acoustical Society of America*, vol. 119, no. 5, pp. 2815–2825, 2006.

[11] C. Richard, D. Guyomar, D. Audigier, and G. Ching, “Semi-passive damping using continuous switching of a piezoelectric device,” in *SPIE proceedings series*, pp. 104–111.

[12] C. Richard, D. Guyomar, D. Audigier, and H. Bassaler, “Enhanced semi-passive damping using continuous switching of a piezoelectric device on an inductor,” in *Society of Photo-Optical Instrumentation Engineers (SPIE) Conference Series*, 2000, vol. 3989, pp. 288–299.

[13] D. Guyomar and A. Badel, “Nonlinear semi-passive multimodal vibration damping: An efficient probabilistic approach,” *Journal of Sound and Vibration*, vol. 294, no. 1–2, pp. 249–268, Jun. 2006.

[14] M. Lallart, É. Lefeuvre, C. Richard, and D. Guyomar, “Self-powered circuit for broadband, multimodal piezoelectric vibration control,” *Sensors and Actuators A: Physical*, vol. 143, no. 2, pp. 377–382, May 2008.

[15] A. J. Fleming and S. O. R. Moheimani, “Adaptive piezoelectric shunt damping,” *Smart Materials and Structures*, vol. 12, no. 1, pp. 36–48, Feb. 2003.

[16] C. Richard, D. Guyomar, and É. Lefeuvre, “Self-powered electronic breaker with automatic switching by detecting maxima or minima of potential difference between its power electrodes,” 08-Jun-2007. [Online]. Available:http://patentscope.wipo.int/search/en/WO2007063194. [Accessed: 14-Sep-2012].

[17] M. Lallart, C. Magnet, C. Richard, É. Lefeuvre, L. Petit, D. Guyomar, and F. Bouillault, “New Synchronized Switch Damping methods using dual transformations,” *Sensors and Actuators A: Physical*, vol. 143, no. 2, pp. 302–314, May 2008.
[18] W. W. Clark, “Vibration Control with State-Switched Piezoelectric Materials,” *Journal of Intelligent Material Systems and Structures*, vol. 11, no. 4, pp. 263–271, Apr. 2000.
[19] L. Garbuio, D. Guyomar, “Dispositif de correction du facteur de puissance, ” FR 2951836 (A1), (2011)
[20] H. Allik and T. J. R. Hughes, “Finite element method for piezoelectric vibration,” *International Journal for Numerical Methods in Engineering*, vol. 2, no. 2, pp. 151–157, 1970.